DOI: 10.1534/genetics.108.091736

UBIQUITIN-SPECIFIC PROTEASE 26 Is Required for Seed Development and the Repression of *PHERES1* in Arabidopsis

Ming Luo,*[,1,2] Ming-Zhu Luo,[†,1] Diana Buzas,* Jean Finnegan,* Chris Helliwell,* Elizabeth S. Dennis,* W. J. Peacock* and Abed Chaudhury*[,3]

**CSIRO Plant Industry, Canberra, ACT 2601, Australia and [†]College of Agronomy, South China Agricultural University, Guangzhou 510624, China*

Manuscript received May 19, 2008
Accepted for publication July 1, 2008

ABSTRACT

The Arabidopsis mutant *Atubp26* initiates autonomous endosperm at a frequency of ~1% in the absence of fertilization and develops arrested seeds at a frequency of ~65% when self-pollinated. These phenotypes are similar to those of the *FERTILIZATION INDEPENDENT SEED* (*FIS*) class mutants, *mea*, *fis2*, *fie*, and *Atmsi1*, which also show development of the central cell into endosperm in the absence of fertilization and arrest of the embryo following fertilization. *Atubp26* results from a T-DNA insertion in the *UBIQUITIN-SPECIFIC PROTEASE* gene *AtUBP26*, which catalyzes deubiquitination of histone H2B and is required for heterochromatin silencing. The paternal copy of *AtUBP26* is able to complement the loss of function of the maternal copy in postfertilization seed development. This contrasts to the *fis* class mutants where the paternal *FIS* copy does not rescue aborted seeds. As in the *fis* class mutants, the Polycomb group (PcG) complex target gene *PHERES1* (*PHE1*) is expressed at higher levels in *Atubp26* ovules than in wild type; there is a lower level of H3K27me3 at the *PHE1* locus. The phenotypes suggest that AtUBP26 is required for normal seed development and the repression of *PHE1*.

IN angiosperms, fertilization of the egg and central cell nuclei in the embryo sac by the two sperm nuclei is essential for the formation of embryo and endosperm. The development of the embryo, endosperm, and seed coat is coordinated and controlled by both genetic and epigenetic processes (reviewed by Berger *et al.* 2006). The breakdown of coordinated development in some mutant lines is shown by endosperm development in the absence of fertilization when any of the four genes, *MEA*, *FIS2*, *FIE*, and *AtMSI1* are not functional in Arabidopsis. The *FIS* genes encode homologs of the Drosophila Polycomb group (PcG) proteins, members of an epigenetic repressive complex PRC2 (Grossniklaus *et al.* 1998; Luo *et al.* 1999; Ohad *et al.* 1999; Kohler *et al.* 2003a). Loss of function in any of the genes leads to the formation of diploid autonomous endosperm derived from the central cell nucleus in the absence of fertilization. When the mutants are fertilized, the maternal genotype determines the fate of the seed irrespective of the paternal genotype. An ovule carrying a *fis* mutant allele develops into an arrested seed with an arrested embryo and noncellularized endosperm whereas an ovule carrying a wild-type allele develops a viable seed.

The FIS PcG complex mediates the addition of the repressive mark H3K27me3 to the target gene *PHE1* through the histone methyltransferase activity of MEA (Makarevich *et al.* 2006). A mutation in the *MEA* gene reduces the level of H3K27me3 at *PHE1* and leads to increased expression of *PHE1* (Makarevich *et al.* 2006). *PHE1* expression is also elevated in other mutants of the *fis* PcG genes (Kohler *et al.* 2003b). It has been speculated that the FIS complex may have functions before and after fertilization as *fis* mutants have phenotypes in both nonfertilized and fertilized ovules (Sørensen *et al.* 2001; Makarevich *et al.* 2006).

To obtain other mutants with autonomous endosperm development, we screened for arrested embryo and noncellularized endosperm in a small collection of T-DNA insertion lines (http://www.arabidopsis.org) and checked for autonomous seed development following emasculation. We isolated one mutant that had a weak autonomous endosperm phenotype and arrested seed development. The T-DNA insertion caused the loss of function of a H2B deubiquitinating enzyme, AtUBP26 (Sridhar *et al.* 2007) and resulted in mutant seed phenotypes. *PHE1* was upregulated in the mutant ovules and there was a reduced level of H3K27me3 at the *PHE1* locus suggesting that AtUBP26 is required for addition of H3K27me3 at *PHE1* and that AtUBP26 may be necessary for FIS PcG action in seeds.

MATERIALS AND METHODS

Mutant identification, materials, and growth condition: A small collection of Salk lines from the Arabidopsis Stock

[1]These authors contributed equally to this work.

[2]*Corresponding author:* CSIRO Plant Industry, GPO Box 1600, Canberra, ACT 2601, Australia. E-mail: ming.luo@csiro.au

[3]*Present address:* Vitagrain, Uttara Model Town, Dhaka, Bangladesh.

Center was screened for shriveled seeds that resembled *fis* fertilized seeds (Chaudhury *et al.* 1997) (http://www.arabidopsis.org). A putative mutant which produced shriveled seeds was backcrossed to Columbia (Col) to cross out any other T-DNA insertions in the same line. An allele of *mea* (*fis1*, Chaudhury *et al.* 1997), was emasculated to compare the autonomous endosperm development with that of the putative mutant.

The Arabidopsis ecotypes used in this study were Landsberg *erecta* (L*er*) and Col. Two T-DNA insertion lines, Salk_024392 and CS826614 (SAIL_621_F01), which have T-DNA insertions in At3g49600, were obtained from the Arabidopsis Biological Resource Center and confirmed by PCR.

Plants were grown in pots with compost soil under continuous artificial light at 20° in growth chambers. The artificial light was achieved by using an incandescent light source producing a fluence of 180 micro-E for most of the experiments.

Cloning of *AtUBP26* and expression analysis: For mapping, the homozygous mutant plant was crossed as a pollen donor to L*er*. The following SSLP markers located on different part of the chromosomes were used to test F_2 plants: nga63, nga111, nga361, nga172, CIW4, CIW6, and NGA151 (http://www.arabidopsis.org). The recombination frequency between markers and seed phenotypes was scored. Further detailed mapping was done by using the following insertion-deletion (indel) markers on chromosome III on the basis of sequence differences between Col and L*er* (http://www.arabidopsis.org). They are T32N15 FR with primers 5′-AGCTAGGGTTTGGCAAC ATT-3′ and 5′-CTTTTGTGCACGACGGAATCT-3′, T21J18 FR with primers 5′-GCTTTCAAAATTGCTGGAAAA-3′ and 5′-TCA GGCTGCATTAGGCTCTT-3′, F2K15FR with primers 5′-GAA TCAGGTTTGAATAAAATGGAA-3′ and 5′-TTCAATCCTCCAA AATTATCAACA-3′, and T16K5FR with primers 5′-GCGTGA TCATGGAAATATTGG-3′ and 5′-AGCAAGGTTATGCATTTC AGA-3′. The genotypes of each plant for the SSLP and indel markers were visualized on 4% agarose gel. The plant DNA preparation and the PCR reactions were carried out as described by Bell and Ecker (1994).

For isolating T-DNA border sequences, DNA was extracted using a QIAGEN DNeasy mini kit. T-DNA border isolation and sequencing were carried out as described (http://signal.salk.edu/). Primers used to amplify T-DNA junctions were LBb1, 5′-GCGTGGACCGCTTGCTGCAAC-3′ and *AtUBP26* TF2, 5′-TCGTTAATCGGAATCAAAATTG-3′. Individual plants of the mapping F_2 population were PCR amplified with LBb1 and *AtUBP26* TF2.

For complementation, a genomic fragment including promoter and coding region was generated by PCR and fused to FLAG in vector pCH252 (Helliwell *et al.* 2006) using the Gateway recombination system. The primer sequences used were GGGGACAAGTTTGTACAAAAAAGCAGGCTTAATCTG GTGTGATGGAATTGATC and GGGGACCACTTTGTACAAG AAAGCTGGGTAGCAGGCTTCAGAAGAGATATTGGG. Wild-type Col was transformed by floral dip (Clough and Bent 1998). Stable transgenic plants were screened by Western blots with anti-FLAG (Sigma). Homozygous progeny of three independent transgenic plants, which produced the hybrid protein of expected size, were selected to cross to the *Atubp26-2* homozygote. The arrested seeds were scored in the F_1 plants between *Atupb26-2* and the transgenic plants. The arrested seeds were also scored in the F_1 plants of a control cross between *Atubp26-2* and Col.

RT–PCR was performed on RNA isolated from buds, cauline leaves, rosette leaves, young seedlings, seeds 3 days postfertilization, embryos 7 days postfertilization, endosperm 7 days postfertilization, young siliques 1–2 days postfertilization, and stems using a Promega Access RT–PCR system kit. Primers used for *AtUBP26* are 5′-CATTGCAGCTTCCACA AAAA-3′ and 5′-TGCTTTTGTCAAGACGTTGG-3′. For the control gene *FORMALDEHYDE DEHYDROGENASE* (*FDH*), primers 5′-TGGGAAACCCATTTATCACTTCA-3′ and 5′-CAG CAAGTCCAACAGTGCCAAG-3′ were used (Luo *et al.* 2005).

Microscopy: Fertilized and unfertilized siliques were dissected under a dissecting microscope. Developing seeds were cleared (Boisnard-Lorig *et al.* 2001). Specimens were examined with a Leica (Deerfield, IL) microscope using differential interference contrast optics. Mature seeds of Col, *Atubp26-2*, *Atubp26-3*, and *Atubp26-4* were photographed and captured as digital images under a dissection microscope.

Real-time PCR: RNA was isolated from young siliques 36, 60, and 84 hr postfertilization from both *Atubp26-2* and Col, using a QIAGEN RNeasy plant mini kit with Dnase I treatment according to the manufacturer's protocol. RNAs were also harvested from rosette leaves and buds from both *Atubp26-2* and Col. Silique RNAs 84 hr postfertilization from L*er* and *mea* (*fis1*, Chaudhury *et al.* 1997) were isolated. Approximately 3 μg total RNA was used for cDNA synthesis using an Invitrogen Superscript III reverse transcriptase kit. Real-time PCR was performed using *PHE1* primers by following Kohler *et al.* (2003b). *FDH* primers were used as internal control (Luo *et al.* 2005). For each stage, at least three biological repeats were conducted.

Real-time PCRs were also performed on cDNAs from young silique 84 hr postfertilization for both *Atubp26-2* and Col with *MEA*, *FIS2*, *FIE*, and *AtMSI1*.

Chromatin immunoprecipitation: Chromatin immunoprecipitation (Johnson *et al.* 2002) was carried out using an antibody against histone H3K27me3 (Upstate). Buds (including all the tips without open flowers) and siliques 60–84 hr postfertilization were harvested for chromatin preparation. After chromatin immunoprecipitation, DNA was used for real-time PCR using primers amplifying region 2 of the *PHE1* locus described by Makarevich *et al.* (2006). For an internal control, we used primers 5′-CCCAAAGATTTTAGTGCCTCA-3′ and 5′-GGTTCAAGAGGGCAATCAC-3′ from the 5′-UTR of *AG* described by Finnegan and Dennis (2007). This region has been shown to be enriched by the H3K27me3 antibody (Schubert *et al.* 2006). *AG* gene expression was not affected in the *Atubp26* mutant at bud or silique stage. Thus the *AG* 5′-UTR is a suitable control in our experiment. Three pull-down experiments have been carried out for both stages. DNA precipitated by H3K27me3 antibody was normalized with the 5′-UTR of *AG*. We calculated the relative enrichment and statistical analysis as described by Finnegan and Dennis (2007).

RESULTS

T-DNA insertions in *Atubp26*, a ubiquitin-specific protease gene, cause arrested seed phenotypes: In a screen of ~200 T-DNA insertion lines, 20 lines with a proportion of shriveled seeds were identified. Two shriveled seeds coming from one line, Salk_014298, germinated on an MS plate while the shriveled seeds from other lines failed to germinate. The resulting plants displayed short siliques and produced ~60% shriveled seeds with arrested embryos (Figure 1, A–D). These seed phenotypes are similar to those of the *FERTILIZATION INDEPENDENT SEED* (*FIS*) class mutants, *mea*, *fis2*, *fie*, and *Atmsi1* (Chaudhury *et al.* 1997; Grossniklaus *et al.* 1998; Ohad *et al.* 1999; Kohler *et al.* 2003a). As the Salk_014298 line is known to have a T-DNA insertion in the gene *ITB1* (At2g35110) and *itb1* does not display any seed phenotype (Zhang *et al.* 2005), the seed pheno-

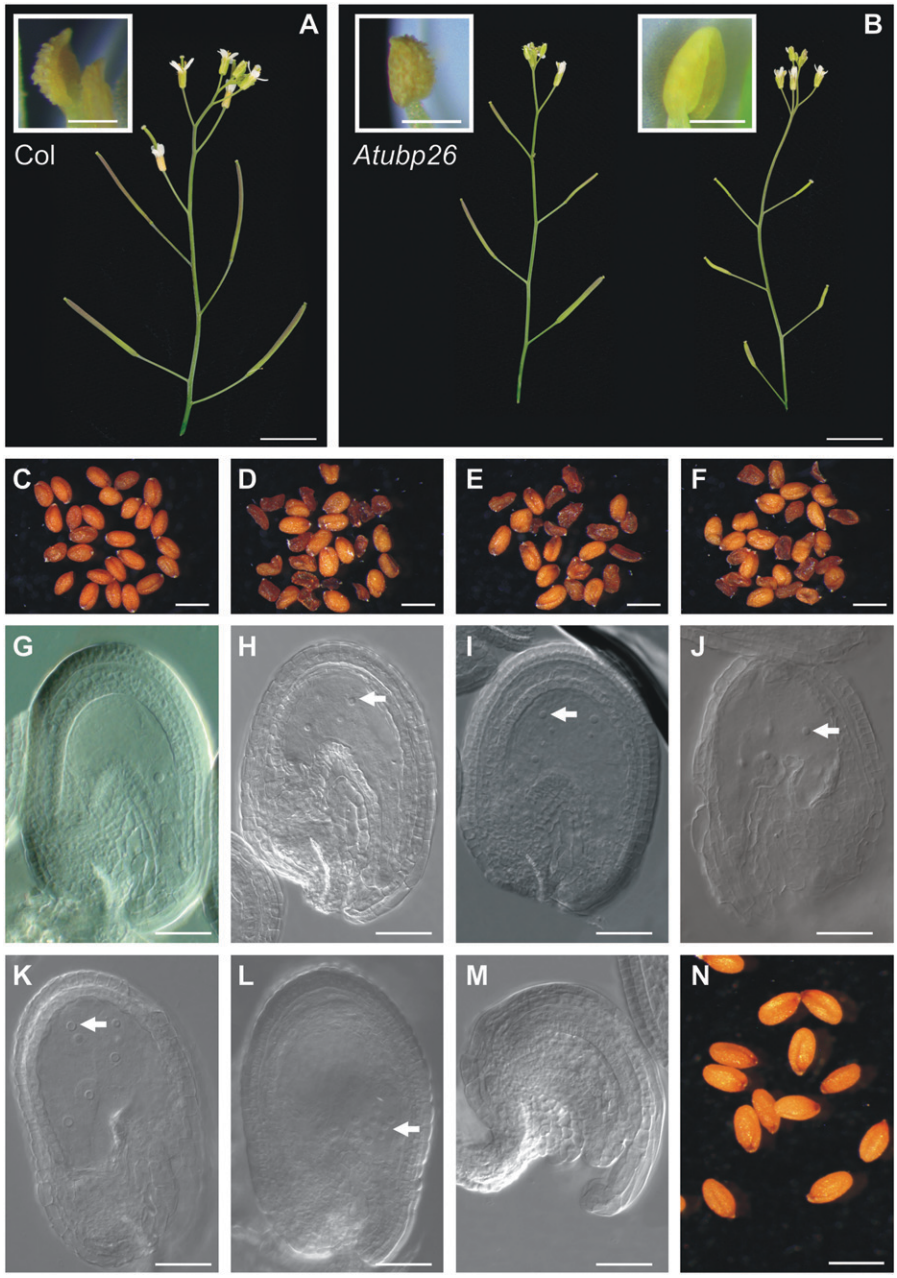

Figure 1.—Phenotypes of *Atubp26*. (A) Col wild type with fertile flowers and elongated siliques. Inset is an anther with pollen grains. (B) Siliques on an early-emerged branch (left) are longer than that of a late-emerged branch (right) in *Atubp26-2* due to the lack of dehiscent anthers. Right inset shows a nondehiscent anther from an open flower in a late-emerging branch. Left inset shows a dehiscent anther from a *Atubp26-2* homozygote from an open flower in an early-emerging branch. (C) Col mature seeds. (D) *Atubp26-2* homozygote seeds showing both full and shriveled seeds. (E) *Atubp26-3* homozygote seeds. (F) *Atubp26-4* homozygote seeds. (G) An unfertilized ovule 7 days postemasculation in Col showing a fused central-cell nucleus. (H) An *Atubp26-2* unfertilized ovule with six endosperm nuclei (two out of focus). (I) An *Atubp26-3* unfertilized ovule with four endosperm nuclei. (J) An *Atubp26-4* unfertilized ovule with endosperm nuclei (some out of focus). (K) An unfertilized ovule with endosperm nuclei of an *Atubp26-2* heterozygote in the *ap3/ap3* background. (L) An unfertilized ovule with endosperm nuclei of an *Atubp26-2* heterozygote in the *ap3/ap3* background. Note that the nuclei are concentrated at the micropylar region. (M) An *Atubp26-2* aborted ovule with no developed embryo sac. (N) An *Atubp26-2* homozygote pollinated with wild-type pollen showing viable seeds. Arrows in H–L indicate the endosperm nuclei. Bars in A and B, 10 mm; C–F and N, 0.5 mm; G–M, 0.1 mm.

type segregated away from the *itb* mutation in a backcross to Col.

We established a F_2 mapping population between L*er* and the mutant. F_1 plants did not display 50% shriveled F_2 seeds as do the *fis* class mutants *mea*, *fis2*, *fie*, and *Atmsi1*; instead they produced 14/120 shriveled F_2 seeds. The selfed progeny from the two original plants did not contain any wild-type plants but displayed a uniform arrested seed phenotype, indicating that the original plants were homozygous mutants. The mutation was closely linked to the SSLP marker CIW4 and located on the bottom of chromosome 3 in a 240-kb region in which no *fis* class mutations have been found (Figure 2A).

We isolated the junction sequences of T-DNA insertions from 14 plants derived from the original mutant plants. T-DNAs were inserted in three different genes, At2g35110, At3g49600, and At1g69870. At2g35110 is the *ITB1* gene; At3g49600 is located in the same region as the new mutant (Figure 2A), suggesting that At3g49600 may be the locus mutated. PCR primers that specifically amplified the T-DNA junction in At3g49600 were used to test a total of 260 plants heterozygous for the mutation and 20 wild-type plants in the F_2 of Col crossed with the original mutant. The T-DNA insertion cosegregated with the shriveled seed phenotype. To confirm that the T-DNA insertion in At3g49600 causes the mutant phenotype, we obtained additional T-DNA insertion lines,

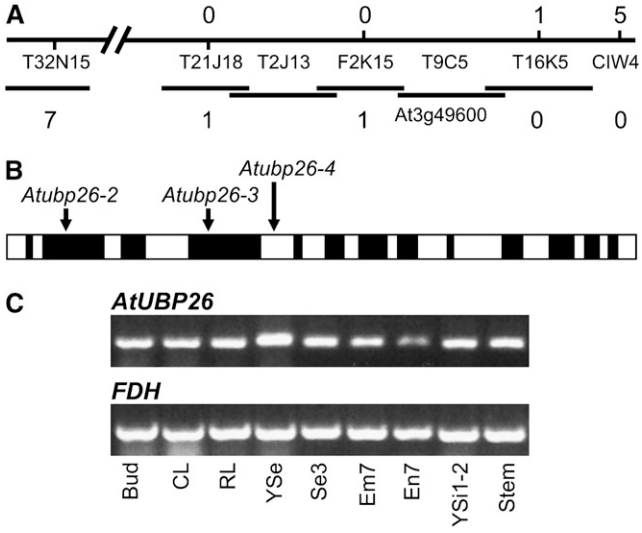

FIGURE 2.—Mapping and expression of *AtUBP26*. (A) The mutant gene was mapped to a contig containing At3g49600/*AtUBP26*. Markers CIW4 and T16K5 FR were used to identify five and one recombinants, respectively, which showed crossovers between the mutant locus and the markers. Markers T32N15 FR, T21J18 FR, and F2K15 FR identified seven, one, and one recombinants, respectively. (B) Schematic of *AtUBP26* showing the T-DNA insertions in three alleles. Solid boxes represent exons and open boxes, introns. (C) RT–PCR showing that *AtUBP26* is expressed in buds, cauline leaves (CL), rosette leaves (RL), young seedlings (YSe), seeds 3 days postfertilization (Se3), embryos 7 days postfertilization (Em7), endosperm 7 days postfertilization (En7), young siliques 1–2 days postfertilization (YSi1-2), and stems.

Salk_024392 and CS826614, in which At3g49600 is interrupted (Figure 2B). Both alleles gave shriveled seeds and autonomous endosperm development (Figure 1, E, F, I, and J). These mutant alleles failed to complement each other, suggesting that the T-DNA insertions in At3g49600 cause the mutant seed phenotype. At3g49600 encodes a UBIQUITIN-SPECIFIC PROTEASE and has previously been designated *AtUBP26* (YAN *et al.* 2000). *Atubp26-2* has a T-DNA insertion in the second exon, *Atubp26-3* in the fourth exon, and *Atubp26-4* in the fifth intron (Figure 2B). The positions of the T-DNA insertions suggest that all the alleles are null mutants.

We further confirmed by complementation that the *AtUBP26* is the gene responsible for the phenotype. Three independent transgenic homozygotes carrying a wild-type allele-FLAG fusion were crossed to *Atubp26-2*. Five mature siliques were scored to determine the frequency of arrested seeds in each plant. Five plants were investigated for each F_1 population. F_1 plants with the transgene showed a reduced frequency of arrested seeds (Table 1) in contrast to the control F_1 plants, which produced ~13% arrested seed. This result showed that the transgene complemented the lesion caused by the *Atubp26-2* mutation.

AtUBP26 is expressed in buds, cauline leaves, rosette leaves, young seedlings, seeds 3 days postfertilization, embryos 7 days postfertilization, endosperm 7 days postfertilization, young siliques 1–2 days postfertilization, and stems (Figure 2C) consistent with the results of SRIDHAR *et al.* (2007). MPSS data also suggest that *AtUBP26* is expressed in inflorescences, siliques, roots, and leaves (http://mpss.udel.edu/at/).

Loss of *Atubp26* leads to endosperm initiation at low frequency in the absence of fertilization: Both homozygous *Atubp26-2* and Col siliques were slightly elongated after emasculation. In wild-type Col, no ovules showed division of the central cell nucleus (of a total of 1200 ovules checked) (Figure 1G). Approximately 1% (16/1200) of the ovules in *Atubp26-2* became slightly enlarged and showed autonomous division of the central cell nucleus (Figure 1H). Most cases of autonomous endosperm development in *Atubp26-2* only reached the 4- to 8-nuclei stage ($n = 13$) but in a few ovules the endosperm developed beyond 8 nuclei ($n = 3$). *Atubp26-3* and *Atubp26-4* showed similar autonomous seed phenotypes (Figure 1, I and J; Table 2). In contrast to *Atubp26*, 10–15% of ovules of a *mea* (*fis1*) allele were enlarged and most developed autonomous endosperm with >20 nuclei.

To investigate whether the autonomous phenotype is determined by the genotype of the embryo sac or the maternal somatic tissue, we emasculated heterozygous *Atubp26-2* plants (in a Col background). Autonomous development of the central cell was observed. We reconfirmed that the autonomous endosperm initiation occurred in heterozygous *Atubp26-2* using an *ap3/ap3*

TABLE 1

The frequency of arrested seeds in F_1 plants

	Atubp26 × Col	*Atubp26* × tra*1	*Atubp26* × tra 2	*Atubp26* × tra 3
Plant1	40/305 (13)	4/310 (1.3)	5/275 (1.8)	10/312 (3.2)
Plant2	40/300 (13)	7/305 (2.2)	8/285 (2.8)	8/313 (2.6)
Plant3	40/295 (13)	6/290 (2.1)	9/295 (3.1)	7/250 (3.4)
Plant4	38/280 (14)	4/275 (1.5)	8/300 (2.6)	6/270 (2.9)
Plant5	35/275 (12)	6/305 (2)	7/311 (2.3)	4/290 (1.4)
Average %	13	1.82	2.52	2.7

tra*, Col carrying a construct of wild-type allele of *AtUBP26-FLAG*. Numbers in parentheses are percentages.

TABLE 2

Ovule and seed phenotypes of *Atubp26-2*

	Multiple nuclei after emasculation	Aborted ovules	Aborted seed ratio			Full seeds
			Globular	Globular heart	Torpedo	
Wild type	0/1200	2/310 (0.65)		None		308/310 (99.35)
Atubp26-2 homozygote	16/1200 (1.3)	48/240 (20)	15/240 (6.3)	62/240 (25.8)	35/240 (14.6)	80/240 (33.3)
Atubp26-2 heterozygote	4/900 (0.44)	4/450 (0.89)	9/450 (2)	35/450 (7.8)	17/450 (3.8)	385/450 (85.6)
Atubp26-3 homozygote	3/350 (0.86)	17/100 (17)	5/100 (5)	30/100 (30)	12/100 (12)	36/100 (36)
Atubp26-4 homozygote	2/270 (0.74)	16/105 (15.2)	5/105 (4.8)	34/105 (32.4)	10/105 (9.5)	39/105 (37.1)

Numbers in parentheses are percentages.

male sterile plant (Figure 1, K and L; Table 2). Sometimes, the autonomous endosperm nuclei congregated at the micropylar end (Figure 1L) where the earliest endosperm divisions take place.

***AtUBP26-2* has an arrested embryo phenotype following fertilization:** In homozygous *Atubp26-2* plants, 20% (48/240) of ovules failed to form seeds upon self-pollination, resulting in slightly shorter siliques than in wild type (Figure 1, A and B). These ovules did not develop an embyo sac (Figure 1M). Late-developing branches set even fewer seeds (Figure 1B) and gave short siliques. In newly opened flowers on branches with short siliques most of the anthers had not opened, in contrast to wild-type flowers at the same stage in which released pollen grains could be seen (Figure 1, A and B insets). Flowers on late branches responded to pollination with wild-type pollen as did some of the flowers in early branches. Thus the partial sterility could be caused by either or both the lack of pollen from nondehiscent anthers and the lack of embryo sacs in *Atubp26-2*. We tested whether transmission of the mutant gene by pollen had been affected by pollinating wild-type with pollen from a heterozygote plant. There were 55 heterozygote mutants and 48 wild-type plants among the progeny, indicating that mutation in *AtUBP26* does not affect pollen viability.

While 20% of ovules failed to develop embryo sacs, 80% (192/240) of ovules give seeds upon fertilization. In self-fertilized *Atubp26-2* seeds (240 − 48 = 192), 58.4% (112/192) of the resulting seeds were arrested at various stages of development and 41.6% (80/192) of seeds developed fully (Table 2; Figure 1D). When *Atubp26-2* was pollinated with wild-type pollen, all the seeds developed fully (Figure 1N). Thus, the paternal wild-type *AtUBP26* can fully complement the loss of function of the maternal *Atubp26* allele. In *fis* class mutants the maternal gametophyte genotype determines the seed phenotype irrespective of the paternal contribution (Chaudhury *et al.* 1997; Grossniklaus *et al.* 1998; Ohad *et al.* 1999; Kohler *et al.* 2003a).

We did not see any other abnormal morphology in *Atubp26* homozygotes. The heterozygote of *Atubp26-2* set 61/450 (15%) arrested seeds upon self-pollination and did not have the unopened anthers seen in the *Atubp26-2* homozygote. There were some aborted ovules but at a level comparable to wild type (Table 2). In contrast, heterozygous *mea*, *fis2*, *fie*, and *Atmsi1* displayed 50% arrested seeds when self-pollinated or pollinated with wild-type pollen as expected for a locus operating in the gametophyte.

We characterized the defects in the self-pollinated *Atubp26-2* seeds by analyzing the early seed morphology of the mutant and wild type using cleared whole seeds (Boisnard-Lorig *et al.* 2001). Seed arrested 32.2% (62/192) at heart stage (Figure 3, G and H), 7.8% (15/192) at the globular stage (Figure 3F), 18.2% (35/192) beyond heart stage (Figure 3I), while 41.6% (80/192) of embryos developed fully. Fully developed seeds showed 100% ($n = 80$) germination. Early embryo development up to the globular stage is similar in *Atubp26-2* and wild type (Figure 3, A–E). The wild-type endosperm was cellularized at heart stage (Figure 3C), whereas all the arrested embryos were associated with un-cellularized endosperm ($n = 112$; Figure 3, F–H). Seeds in Figure 3, G and H, showed overproliferated endosperm with 710 and 750 nuclei, respectively, while the same stage wild-type endosperm had only 410 ± 30 nuclei ($n = 2$). We also observed an enlarged chalazal cyst in some mutant seeds (Figure 3H). The two other *Atubp26* alleles showed similar seed abortion and embryo arrest frequencies (Table 2). The seed-arrested phenotype in the heterozygote is similar to that in the homozygote, indicating that there is no maternal sporophytic effect on seed development in the mutant (Figure 3, J and K; Table 2).

AtUBP26 regulates *PHE1* expression: *PHE1*, a type I MADS-box gene was upregulated relative to wild type (Kohler *et al.* 2003b) in *mea*, *fis2*, and *fie* young siliques. Given that *Atubp26-2* displayed phenotypes similar to the *fis* mutants, we tested whether *PHE1* was upregulated in developing siliques. Because *PHE1* has a similar sequence to *PHE2* (Kohler *et al.* 2003b), we confirmed that the RT–PCR products were specific for *PHE1* by sequencing 18 subclones. *PHE1* expression was signifi-

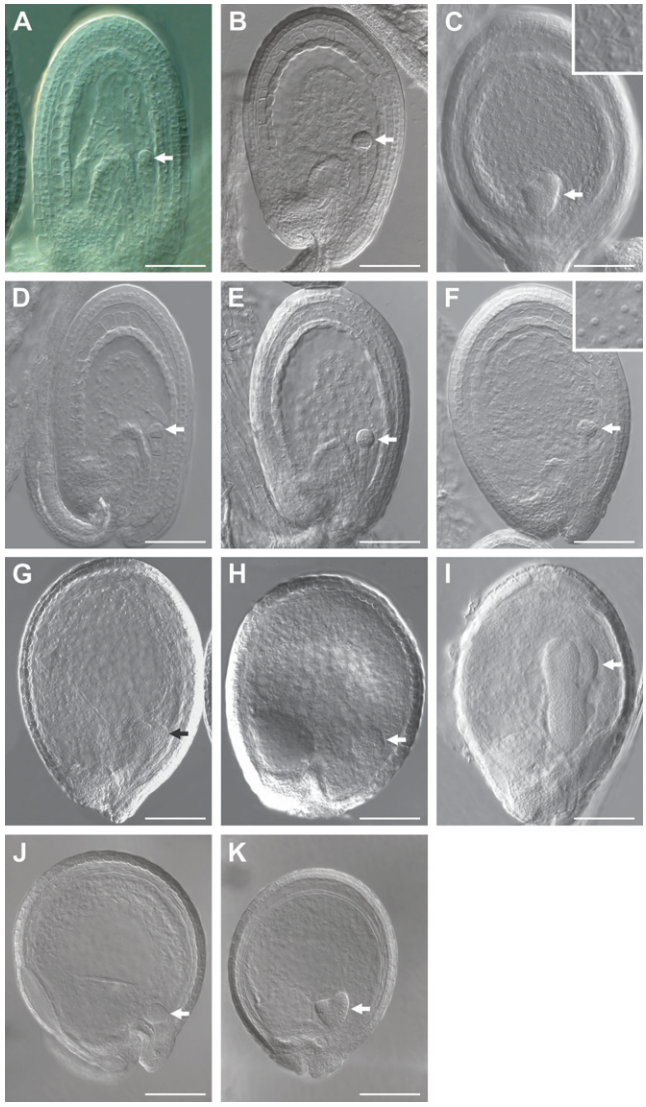

FIGURE 3.—*Atubp26* aborted seed phenotypes. (A–C) Embryo and endosperm development in wild-type seeds at 48, 72, and 96 hr postfertilization. In A and B, globular embryos and syncytial endosperm were observed. In C, heart-stage embryo and cellularized endosperm were observed. (Inset) Cell wall of endosperm. (D and E) *Atubp26* seeds at 48 and 72 hr showing similar development to wild type of the same age. (F) An *Atubp26* seed at 96 hr containing an arrested globular embryo and syncytial endosperm. (Inset) Free endosperm nuclei. (G and H) *Atubp26* seeds at 120 hr containing arrested heart or globular embryo and syncytial endosperm. (I) An *Atubp26* seed at 120 hr containing a torpedo stage embryo. (J) Seed with arrested globular embryo from a heterozygote. (K) Seed with arrested heart embryo from a heterozygote. Arrows indicate the embryos. Bars in A, B, D, and E are 50 μm; in C, F, and G–I are 0.1 mm.

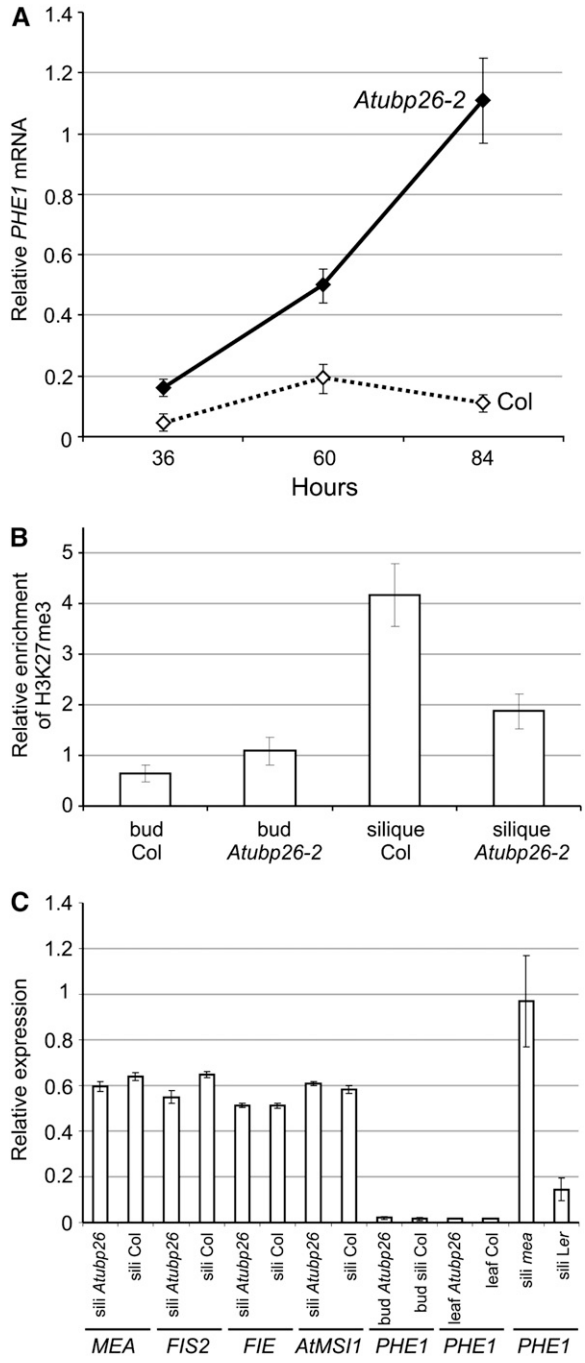

FIGURE 4.—*PHE1* expression is elevated in *Atubp26* siliques. (A) Real-time PCR showing *PHE1* expression in *Atubp26* and wild-type siliques at 36, 60, and 84 hr postfertilization. (B) Chromatin immunoprecipitation analysis of H3K27me3 at the *PHE1* locus. There was a higher enrichment of the *PHE1* region in Col than in *Atubp26* siliques (60–84 hr old) after chromatin immunoprecipitation using a H3K27me3 antibody but no difference in buds. (C) *MEA*, *FIS2*, *FIE*, *AtMSI1*, and *FWA* expression in *Atubp26* and wild-type siliques of 2–3 days; *PHE1* expression in *Atubp26* and wild-type leaves; *PHE1* expression in *mea* and wild-type siliques of 2–3 days.

cantly increased compared to the control Col in RNA extracted from 36-hr- (mainly containing early globular embryos), 60-hr- (globular embryos), and 84-hr- (late globular and heart-stage embryo) old siliques of *Atubp26-2* and Col (Figure 4A). We also observed increased expression of *PHE1* in *mea*. *PHE1* expression in buds and leaves is very low and was not elevated in the mutant (Figure 4C). At late globular and heart stage, the *PHE1* mRNA level was up to ninefold higher in *Atubp26-2* siliques than in wild type (Figure 4A). In early stages,

there was a two- to threefold increase of *PHE1* expression in *Atubp26-2* siliques compared with wild-type siliques. The upregulation of *PHE1* could be caused indirectly by a reduction in expression of *FIS* class genes if *AtUBP26* were a positive regulator of *FIS* genes. We did not find any reduction of expression of *MEA*, *FIS2*, *FIE*, and *AtMSI1* in 60-hr-old siliques of *Atubp26-2* compared to Col (Figure 4C). We conclude that *AtUBP26* regulates *PHE1* in developing seed but does not regulate the *FIS* class genes.

H3K27me3 is reduced at *PHE1* chromatin in *Atubp26* young siliques: Repression of *PHE1* expression is associated with increased H3K27me3 at the *PHE1* locus, which is dependent on the histone methyltranferase activity of MEA (Kohler *et al.* 2003b; Makarevich *et al.* 2006). As shown above, *PHE1* expression was elevated in *Atubp26-2* siliques. In these siliques, H3K27me3 was reduced to half the wild-type level at the *PHE1* locus, suggesting that AtUBP26 is required to maintain H3K27me3 at the *PHE1* locus (Figure 4B).

We did not observe any difference in the level of H3K27me3 at the *PHE1* locus in buds of *Atubp26-2* and Col wild type (Figure 4B).

DISCUSSION

Lack of activity of *AtUBP26*, which catalyses the deubiquitination of H2B (Sridhar *et al.* 2007), causes low frequency autonomous endosperm growth without fertilization and embryo arrest if self-pollinated. The mutant seed phenotypes of *Atubp26* are similar to those of the *fis* class mutants *mea*, *fis2*, *fie*, and *Atmsi1* suggesting that *AtUBP26* may act, at least in part, in the same pathway as the *FIS* genes. We consistently observed a lower frequency of autonomous endosperm development in the three alleles of *Atubp26* than in *fis* class mutants. Autonomous endosperm rarely develops beyond 16 nuclei in *Atubp26*, while in the mutant *mea*, autonomous endosperm may produce >20 nuclei. The observation of low-frequency autonomous development of the central cell in *Atubp26* heterozygotes suggests that this phenotype is under gametophytic control with low penetrance.

The weaker autonomous endosperm phenotype in *Atubp26* is paralleled by its weaker postfertilization phenotype. When homozygous, all three alleles of *Atubp26* formed ~40% viable seeds following self-pollination while *mea* and *fis2* homozygotes produce <1% viable seed. The low penetrance of the autonomous endosperm phenotype in *Atubp26* is unlikely to be due to a partially functioning *Atubp26* gene because all three alleles are likely to be null mutations as the T-DNA insertions are in exons. *AtUBP26* may be redundant with other *UBP* genes as there are 27 genes identified encoding UBPs in the Arabidopsis genome. *AtUBP26* is the only one in its class (Yan *et al.* 2000) but other genes may be able to partially complement the loss of AtUBP26. In the *Atubp26* mutant, the level of ubiquitinated histone H2B is only slightly increased over that in wild type (Sridhar *et al.* 2007), suggesting that other UBPs may be involved. An alternative explanation of the weak "*fis*" phenotype in *Atubp26* is that the target loci of H2B deubiquitination by AtUBP26 do not completely overlap with the target loci of H3K27 trimethylation by the FIS Polycomb complex; the misregulated genes in the *Atubp26* ovules may not be exactly the same set of genes misregulated in *fis* mutants. We speculate that there are some common target genes, including *PHE1*, which, when derepressed in *Atubp26*, cause a *fis* phenotype. There are at least three genes *PHE1*, *PHE2*, and *MEIDOS* that are upregulated in the *mea* mutant siliques with only *PHE1* having been characterized for its status of histone H3K27 trimethylation in siliques (Kohler *et al.* 2003b; Makarevich *et al.* 2006). In this study, we focused on *PHE1* and showed that *PHE1* expression is elevated in mutant siliques relative to wild type and is accompanied by the loss of H3K27me3 as in a *mea* mutant (Makarevich *et al.* 2006). It remains to be determined whether the other two genes *PHE2* and *MEIDOS* are upregulated and histone-demethylated in the *Atubp26* mutant. In Drosophila, the ubiquitin-specific protease USP7 catalyzes the deubiquitination of H2B and contributes to epigenetic silencing of homeotic genes by PcG proteins. The silencing of USP7 by RNAi causes global reduction of H3K27me3 (van der Knaap *et al.* 2005). Although the mechanism causing this reduction of H3K27me3 remains unknown, one hypothesis is that ubiquitinated H2B prevents the trimethylation of H3K27 by PcG proteins. Our results and the finding in Drosophila suggest that deubiquitination of H2B mediated by UBPs is required for H3K27me3 addition.

Atubp26 and *fis* mutants both have embryo-arrested seeds but display different modes of transmission. When a homozygous *Atubp26* mutant was self-pollinated most seeds were aborted with embryos arrested at the globular or heart stage and the endosperm remained noncellularized as in *fis* class mutants. When pollinated with wild-type pollen, all the seeds developed normally, indicating that the paternal copy of *AtUBP26* fully complements the loss of function of the maternal copy in controlling seed development and that the arrested seed phenotype is under sporophytic control. In contrast to the *Atubp26* mutants, the arrested seed phenotype of the *fis* mutants, which cannot be reversed by wild-type pollen, is completely under gametophytic control (Chaudhury *et al.* 1997; Grossniklaus *et al.* 1998; Ohad *et al.* 1999; Kohler *et al.* 2003a).

It is likely that AtUBP26 has a number of functions in development. The abnormal development of *Atubp26* is not restricted to endosperm and embryo. We observed that pollen dehiscence was affected especially in late branches. There was a proportion of aborted embryo

sacs in the mutant with both factors contributing to the partial sterility of the mutant.

Ubiquitination plays a critical role in target protein degradation but also participates in gene regulation by modifying histones (Hershko 2005). Recent reports indicate that ubiquitinated H2A might be involved in gene silencing and ubiquitinated H2B in gene activation (Henry *et al.* 2003; Kao *et al.* 2004; Wang *et al.* 2004). AtUBP26 acts to remove ubiquitin from ubiquitinated H2B (Sridhar *et al.* 2007). Thus AtUBP26 may act as a repressor, causing gene silencing via chromatin remodeling. It has been reported that, in the *Atubp26* mutant, H3K9 dimethylation is reduced, siRNA-directed DNA methylation is suppressed and heterochromatic silencing is released. H2B deubiquitination by AtUBP26 is thought to play an early and crucial role in heterochromatin formation (Sridhar *et al.* 2007). Here we show that the loss of function of AtUBP26 has effects on seed development similar to the loss of function of the seed development repressors, the FIS PcG proteins, leading to both the autonomous growth of endosperm in the absence of fertilization and arrested embryos with noncellularized endosperm. This suggests that AtUBP26 may have a broad role in chromatin remodeling affecting different aspects of silencing processes such as siRNA-mediated heterochromation formation and the FIS Polycomb repression.

LITERATURE CITED

Bell, C. J., and J. R. Ecker, 1994 Assignment of 30 microsatellite loci to the linkage map of *Arabidopsis*. Genomics **19:** 137–144.

Berger, F., P. E. Grini and A. Schnittger, 2006 Endosperm: an integrator of seed growth and development. Curr. Opin. Plant Biol. **9:** 664–670.

Boisnard-Lorig, C., A. Colon-Carmona, M. Bauch, S. Hodge, P. Doerner *et al.*, 2001 Dynamic analyses of the expression of the HISTONE:YFP fusion protein in *Arabidopsis* show that syncytial endosperm is divided in mitotic domains. Plant Cell **13:** 495–509.

Chaudhury, A. M., L. Ming, C. Miller, S. Craig, E. S. Dennis *et al.*, 1997 Fertilization-independent seed development in Arabidopsis thaliana. Proc. Natl. Acad. Sci. USA **94:** 4223–4228.

Clough, S. J., and A. F. Bent, 1998 Floral dip: a simplified method for *Agrobacterium*-mediated transformation of *Arabidopsis thaliana*. Plant J. **16:** 735–743.

Finnegan, E. J., and E. S. Dennis, 2007 Vernalization-induced trimethylation of histone H3 lysine 27 at FLC is not maintained in mitotically quiescent cells. Curr. Biol. **17:** 1978–1983.

Grossniklaus, U., J. P. Vielle-Calzada, M. A. Hoeppner and W. B. Gagliano, 1998 Maternal control of embryogenesis by MEDEA, a polycomb group gene in Arabidopsis. Science **280:** 446–450.

Helliwell, C. A., C. Wood, M. Robertson, W. J. Peacock and E. S. Dennis, 2006 The Arabidopsis FLC protein interacts directly in vivo with *SOC1* and *FT* chromatin and is part of a high-molecular weight protein complex. Plant J. **46:** 183–192.

Henry, K. W., A. Wyce, W. S. Lo, L. J. Duggan, N. C. Emre *et al.*, 2003 Transcriptional activation via sequential histone H2B ubiquitylation and deubiquitylation, mediated by SAGA-associated Ubp8. Genes Dev. **17:** 2648–2663.

Hershko, A., 2005 The ubiquitin system for protein degradation and some of its roles in the control of the cell division cycle. Cell Death Differ. **12:** 1191–1197.

Johnson, L., X. Cao and S. Jacobsen, 2002 Interplay between two epigenetic marks. DNA methylation and histone H3 lysine 9 methylation. Curr. Biol. **12:** 1360–1367.

Kao, C. F., C. Hillyer, T. Tsukuda, K. Henry, S. Berger *et al.*, 2004 Rad6 plays a role in transcriptional activation through ubiquitylation of histone H2B. Genes Dev. **18:** 184–195.

Kohler, C., L. Hennig, R. Bouveret, J. Gheyselinck, U. Grossniklaus *et al.*, 2003a Arabidopsis MSI1 is a component of the MEA/FIE polycomb group complex and required for seed development. EMBO J. **22:** 4804–4814.

Kohler, C., L. Hennig, C. Spillane, S. Pien, W. Gruissem *et al.*, 2003b The polycomb group protein MEDEA regulates seed development by controlling expression of the MADS box gene *PHERES1*. Genes Dev. **17:** 1540–1553.

Luo, M., P. Bilodeau, A. Koltunow, E. S. Dennis, W. J. Peacock *et al.*, 1999 Genes controlling fertilization independent seed development in Arabidopsis thaliana. Proc. Natl. Acad. Sci. USA **96:** 296–301.

Luo, M., E. S. Dennis, F. Berger, W. J. Peacock and A. Chaudhury, 2005 MINISEED3 (MINI3), a WRKY family gene, and HAIKU2 (IKU2), a leucine-rich repeat (LRR) KINASE gene, are regulators of seed size in Arabidopsis. Proc. Natl. Acad. Sci. USA **102:** 17531–17536.

Makarevich, G., O. Leroy, U. Akinci, D. Schubert, O. Clarenzl *et al.*, 2006 Different polycomb group complexes regulate common target genes in Arabidopsis. EMBO Rep. **7:** 947–952.

Ohad, N., R. Yadegari, I. Margossian, M. Hannon, D. Michaeli *et al.*, 1999 Mutations in FIE, a WD polycomb group gene, allow endosperm development without fertilization. Plant Cell **11:** 407–416.

Schubert, D., L. Primavesi, A. Bishopp, G. Roberts, J. Doonan *et al.*, 2006 Silencing by plant Polycomb-group genes requires dispersed trimethylation of histone H3 at lysine 27. EMBO J. **25:** 4638–4649.

Sørensen, M. B., A. M. Chaudhury, H. Robert, E. Bancharel and F. Berger, 2001 Polycomb group genes control pattern formation in plant seed. Curr. Biol. **11:** 277–281.

Sridhar, V. V., A. Kapoor, K. Zhang, J. Zhu, T. Zhou *et al.*, 2007 Control of DNA methylation and heterochromatic silencing by histone H2B deubiquitination. Nature **447:** 735–738.

van der Knaap, J. A., B. R. P. Kumar, Y. M. Moshkinoshkin, K. Langenberg, J. Krijgsveld *et al.*, 2005 GMP synthetase stimulates histone H2B deubiquitylation by the epigenetic silencer USP7. Mol. Cell **17:** 695–707.

Wang, H., L. Wang, H. M. Erdjument-Bromage, M. Vidal, P. Tempst *et al.*, 2004 Role of histone H2A ubiquitination in Polycomb silencing. Nature **431:** 873–878.

Yan, N., J. H. Doelling, T. G. Falbel, A. M. Durski and R. D. Vierstra, 2000 The ubiquitin-specific protease family from Arabidopsis. AtUBP1 and 2 are required for the resistance to the amino acid analog canavanine. Plant Physiol. **124:** 1828–1843.

Zhang, X., J. Dyachok, S. Krishnakumar, L. G. Smith and D. G. Oppenheimer, 2005 *IRREGULAR TRICHOME BRANCH1* in Arabidopsis encodes a plant homolog of the actin-related protein2/3 complex Activator Scar/WAVE that regulates actin and microtubule organization. Plant Cell **17:** 2314–2326.

Communicating editor: V. Sundaresan